QUANTITATIVE EVALUATION OF CONTRIBUTIONS TO ELECTRON PARAMAGNETIC RESONANCE LINE WIDTHS IN FERRIC HEMOGLOBIN SINGLE CRYSTALS

ARTHUR S. BRILL AND DON A. HAMPTON, *The University of Virginia, Department of Physics, Charlottesville, Virginia 22901 U.S.A.*

ABSTRACT The contributions to the dipolar broadening of ferric magnetic resonances, from crystals of hemoglobin for which the atomic coordinates are known, have been calculated. The total second moment of the $g = 2$ resonance so determined is about 50 $(MHz)^2$ or 5.0 G (peak-to-trough), figures consistent with the range of values found from analysis of experimental data. Two-thirds of this second moment comes from the two protons of the H_2O molecule coordinated to the iron. Treatment with D_2O is predicted to reduce the total second moment at $g = 2$ to about 25 $(MHz)^2$, whereas the experimental measurements on single crystals show no decrease. If the structure of the tetramer is assumed to be the same when in solution as in the crystal, the total second moment is readily redetermined for hemoglobin in solution; the value so obtained is found to be significantly smaller than that from analysis of the $g = 2$ resonance measured in frozen solution. These two unexpected observations can be explained in terms of distributions in spin Hamiltonian parameters, the spread depending upon the nature of the sample—crystal or solution, ordinary or heavy water-treated. This distribution in H_2O and D_2O solutions appears to be about the same, since the measured differences in component line width agree with the calculated difference in dipolar contributions.

INTRODUCTION

Ferric hemoglobin in frozen solution gives an electron paramagnetic resonance (EPR) spectrum with lines significantly broader than those simulated with the widths obtained from single crystal EPR orientation studies of the same protein (Hampton and Brill, 1979). Before offering an explanation of this phenomenon, we want to be able to describe quantitatively those factors that significantly influence the hyperfine component line widths in single crystals of ferric hemoglobin. A detailed treatment of the line broadening interactions of transition metal ion electron spins with the several kinds of protons throughout a crystal has not been given for any protein. Such a treatment is presented below, and the result agrees with experiment. Knowledge of the magnitudes of the separate contributions enables one to identify those sources of line broadening which, when modified, might be expected to alter the observed widths. Consideration of the factors involved leads one to predict that the hyperfine component line widths from ferric hemoglobin in frozen solution will be narrower than in crystals. However, as mentioned above, the observed resonances in frozen solution are broader than in crystals. A spread in spin Hamiltonian parameters,

---

Dr. Hampton's present address is: Alabama Power Company, Birmingham, Ala. 35291.

possibly arising from the freezing in place of an ensemble of conformations, is shown to account for the behavior in solution.

CONTRIBUTIONS TO THE SECOND MOMENT

Ferric Dipoles-Ferric Dipole

The hemoglobin molecule, in crystals and most solutions, is a tetramer consisting of a pair of $\alpha\beta$ dimers. If one focuses upon, say, the ferric ion of a heme group on an α-chain, the dipole-dipole interactions with the other three ferric ions within the molecule are unlikely to depend significantly upon whether it is in a crystal or in solution. The interactions of that α-iron with ferric dipoles in *other* molecules will, of course, differ between crystal and solution, and among solutions of different concentration. Restricting our attention to crystals, we must also recognize the difference between α-irons identical to the one we have focused upon and those that are not identical, because line broadening is treated differently in the two cases. Fig. 1 shows the locations of iron atoms in the monoclinic horse ferrihemoglobin crystal. Within the tetramer, and to nearest neighbors in adjacent molecules, the distances between irons are seen to be in the range 26–36 Å. The α_1 irons constitute one set of identical dipoles, the α_2 irons another such set, etc.

In the Van Vleck point dipoles expression for the second moment of the resonance line (EPR broadening in this case) (Van Vleck, 1948),

$$<\Delta\nu^2_{\lambda\nu}>_j = \frac{1}{3}\frac{S(S+1)}{h^2}\sum_k\left[\frac{3}{2}g^2\mu_B^2\left(\frac{1-3\cos^2\theta_{jk}}{r^3_{jk}}\right)\right]^2 + \frac{1}{3}\frac{S'(S'+1)}{h^2}\sum_{k'}\left[gg_{k'}\mu_B^2\left(\frac{1-3\cos^2\theta_{jk'}}{r^3_{jk'}}\right)\right]^2, \quad (1)$$

the first term on the right gives the contribution from identical sites and the second from the other sites. We employ throughout this analysis a fictitious spin doublet description of the electronic states, with spin $S = S' = \frac{1}{2}$ and effective principal g values of 2.0 normal to the heme plane and about 6.0 in the heme plane. In Eq. 1 the unprimed symbols refer to the sites giving the EPR signal, the primed symbols refer to the other sites, μ_B is the Bohr magneton, θ_{jk} is the angle that the radius vector between the fixed site j and the identical site k makes with the applied magnetic field, r_{jk} is the length of the radius vector, and similarly for $\theta_{jk'}$ and $r_{jk'}$ where site k' is not identical to j. The sums are carried out over the "entire crystal," which from the standpoint of effective contributions to the line width of a central site, computations show can be taken as a sphere of radius 150 Å. Note that the values g and $g_{k'}$ depend upon the angles which the applied field makes with the respective heme normals.

For the α-irons, when the field is in the $g = 2$ direction, Eq. 1 gives 12.1 $(\text{mHz})^2$(2.5 G peak-to-trough)[1], of which 3.7 $(\text{MHz})^2$ comes from within the tetramer. Within the tetramer 3.7 $(\text{MHz})^2$ broadening also applies to the β-irons, but for these sites the contributions from all the irons total 16.5 $(\text{MHz})^2$(2.9 G). On the basis of electron nuclear double reso-

[1]When expressed in gauss, the line width is $2h<\Delta\nu^2>^{1/2}/g\mu_B = 1.43<\Delta\nu^2>^{1/2}/g$. For a Gaussian band, this will be the peak-to-trough line width.

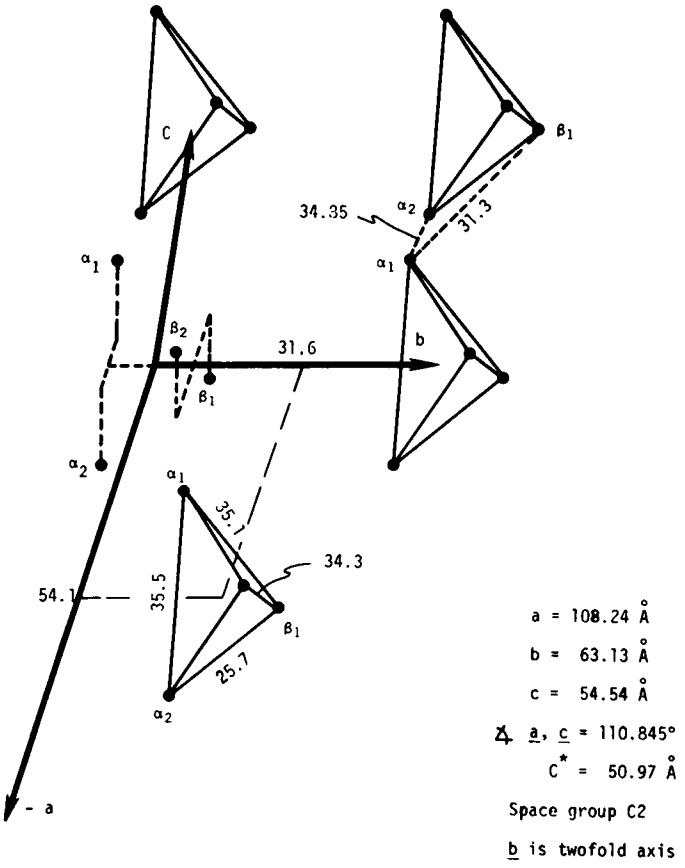

FIGURE 1 Location of iron atoms (•) in neighboring molecules of the horse ferrihemoglobin crystal. (The coordinates upon which this figure is based were supplied by the Medical Research Council Laboratory, Cambridge, England, and can be found in Ladner et al., 1977.)

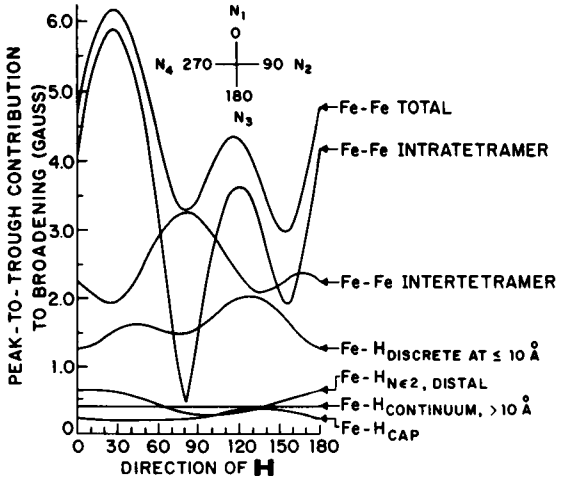

FIGURE 2 Dipolar contributions to line broadening in the $g = 6$ plane of α-chain ferric ions.

nance (ENDOR) measurements on ferric myoglobin (Scholes et al., 1972) and ferric hemoglobin (Feher et al., 1973), a ligand hyperfine splitting of about 2.6 G is expected from the pyrrole nitrogens for the $g = 2$ resonance. The broadening due to iron-iron dipolar interactions alone is seen to make the resolution of EPR nitrogen hyperfine lines marginal in the $g = 2$ directions, and the situation is worse in the $g = 6$ planes, where a similar (about 3 G) superhyperfine splitting is expected. For the α-irons, the ferric-ferric dipolar broadening changes between 160 $(\text{MHz})^2$(3.0 G) and 670 $(\text{MHz})^2$(6.2 G) as the applied magnetic field direction is varied in the heme plane (Fig. 2). Fig. 2 also shows the inter- and intratetramer contributions separately. For the β-irons, the analogous extremes are 130 $(\text{MHz})^2$(2.7 G) and 750 $(\text{MHz})^2$(6.6 G). Because of the similarity of the $g = 6$ planes of the α- and β-irons, a figure for the latter like Fig. 2 is not given here.

Distant (>10 Å) Proton Dipoles-Ferric Dipole

The proton concentrations in protein and mother liquor are 0.051 protons/Å^3 and 0.068 protons/Å^3, respectively.[2] Taking the average concentration to be 0.060/Å^3, one finds the second moment due to a continuum extending from a sphere of radius 10 Å out to infinity to be only 0.3 $(\text{MHz})^2$(0.4 G) for both $g = 2$ and 6 resonances. This calculation is made with the Van Vleck formula as it applies to proton point dipoles:

$$<\Delta\nu_{Av}^2>_j = \frac{1}{3}\frac{I(I+1)}{h^2}\sum_{k'}\left[g\mu_B g_P \beta_N \left(\frac{1-3\cos^2\theta_{jk'}}{r_{jk'}^3}\right)\right]^2. \quad (2)$$

Near (<10 Å) Proton Dipoles-Ferric Dipole, except Coordinated Water Molecule

The three dimensional structures of hemoglobin and myoblobin from X-ray diffraction analysis (Perutz et al., 1968*a*, *b*; Dickerson and Geis, 1969; Ladner et al., 1977) show the heme to be largely surrounded by and in contact with protein groups, except at one edge in open communication with the aqueous phase. We therefore take the mother liquor protons within a sphere of radius 10 Å to occupy a caplike volume over one edge of the heme group, the edge starting 6 Å from the iron. This cap contributes a second moment broadening of 0.2 $(\text{MHz})^2$ (0.3 G) to the $g = 2$ resonance, somewhat less than the contribution of the proton continuum beyond 10 Å. However, the protons on the porphyrin ring and on those sections of the protein that lie within a sphere of radius 10 Å produce about a 30-fold greater contribution to the second moment than the latter two collections of protons. Specifically, a proton point dipole calculation based upon the atomic coordinates of horse ferric hemoglobin[3] and running out to 10 Å gives a second moment of 6.2 $(\text{MHz})^2$(1.8 G) for α-iron and 7.0 $(\text{MHz})^2$(1.9 G) for β-iron at $g = 2$.

---

[2]The masses of the mother liquor constituents (and, hence, the liquor proton density) were determined from pycnometer measurements. The proton density of hemoglobin was calculated from the total number of protons per molecule at neutral pH, and the molecular volume determined from the partial specific volume. The average proton density is the weighted average.

[3]The calculations of this paper utilize atomic coordinates, based upon a 2.8 Å resolution structure (Perutz et al., 1968 *a*, *b*), provided by the Protein Data Bank, Brookhaven National Laboratory, Upton, N.Y. (There are no major differences between this structure and the 2.0 Å resolution structure now available [Ladner et al., 1977].) It should be noted that the porphyrin and protein hydrogen atom coordinates are estimated, since the X-ray diffraction analysis does not provide these directly.

A proton (Nϵ2) on the distal imidazole ring is taken hydrogen-bonded to the water molecule bound to the iron, as it is in the neutron diffraction-determined structure of ferrimyoglobin (Schoenborn, 1971). This proton is close to the ferric ion and also very close to ferric spin delocalized onto the bound water molecule. However, the angular factors and the small amount of spin density on the water are such that the contribution to the second moment from the delocalized spin is small and the broadening is essentially all due to the unpaired spin of the iron. $<\Delta\nu_{Av}^2>$ for this proton is 1.5 (α-iron) and 0.8 (β-iron)(Mhz)^2(0.9 and 0.6 G) for $g = 2$, calculated in a manner similar to that now to be discussed for the protons of the bound water. First, however, note that Fig. 2 gives the $g = 6$ plane interactions of the near protons (exclusive of those on the coordinated water molecule) with α-iron.

Proton Dipoles on Coordinated Water Molecule-Ferric Spin

In its interaction with protons on the bound water molecule, the ferric electronic magnetic moment cannot be taken as a point dipole in a realistic line broadening calculation. For the computations of this paper, the ferric spin (in a fictitious doublet, as before) was distributed in a molecular wave function consisting of a metal ion-localized part, taken to be a Slater orbital, and a delocalized part, taken to be the water orbitals of Ellison and Shull (1955). The classical operator for dipole-dipole interaction leads to a divergent energy when integrated over the volume, which includes zero separation. This divergence at the proton nucleus is handled in the manner of Blinder (1960), Löwdin (1964), and Zhidomirov and Schastnev (1965), with the relativistic correction factor $r/(r + r_0)$; that is, $\mathcal{H}_{dd} = [r/(r + r_0)][-3(\mu_{Fe}\cdot\mathbf{r})(\mu_H\cdot\mathbf{r})/r^5 + \mu_{Fe}\cdot\mu_H/r^3]$, where $r_0 = 1.41 \times 10^{-13}$ cm for the proton. It is not necessary to work with all the components of this expression because, as in the derivation of the point dipole formulae given earlier, only the terms in S_zI_z contribute when the spin eigenstates are $|M_S, M_I>$ (z is the magnetic field direction). However, one must take the S_zI_z coefficient of the entire spin-Hamiltonian for the proton and hence the contact term is to be included. Then

$$<\Delta\nu_{Av}^2> = \frac{1}{3}\frac{I(I+1)}{h^2}\left|<\Psi\left|A + \frac{g\mu_B g_P\mu_N}{5}\frac{r}{r+r_0}\frac{3\cos^2\theta - 1}{r^3}\right|\psi>\right|^2, \quad (3)$$

where A is the coefficient of the contact term and $\psi = \alpha\psi_{Fe} - \alpha'\psi_{ligands}$. If A and α' are set equal to zero, a measure of the second moment from the interaction of the unpaired electrons remaining on the iron with a water proton is obtained. For both protons together, at $g = 2$ this is 22.6 (MHz)^2 (3.4 G) for a water oxygen-iron distance of 2.04 Å. (Curiously, a point ferric dipole generates exactly the same number.) More generally, $g\mu_B g_P\mu_N<\psi_i|[r/(r + r_0)][(3\cos^2\theta - 1)/r^3]|\psi_i>$, when multiplied by the ferric spin in orbital ψ_i, is proportional to the hyperfine field at the proton arising from ψ_i. Provided there is little overlap of the orbitals involved, the sum of these (signed) terms, together with the Fermi term, constitute the expectation value to be used in Eq. 3. For the full calculation we have assumed that the overlap of the water orbitals with the ferric orbital and with each other are of negligible importance, and have taken the delocalized unpaired electrons on the water molecule to be distributed as suggested by Luz and Shulman (1965) for aquo complexes of paramagnetic metal ions: 0.018 in the $\pi_{\text{in plane}}$ ($1b_2$) molecular orbital, 0.04 in the $\pi_{\text{out of plane}}$ ($1b_1$, oxygen $2p_x$) orbital, and very little in the σ molecular orbital. From $1b_1$ plus $1b_2$ there

is a net positive Fermi coupling of 1.2 MHz at each water proton and a dipolar coupling of 0.1 MHz. The contribution to the second moment of the $g = 2$ resonance component line width from one of the water protons is 16.2 $(MHz)^2$, and for both protons, 32.5 $(MHz)^2$ or 4.1 G. If spin is introduced into the σ molecular orbital, the second moment is reduced; for example, 0.06 unpaired electron in the $3a_1$ water orbital drops the moment from 32.5 to 31 $(MHz)^2$.

In the calculation just described, the water oxygen-iron distance was taken as 2.04 Å and the corresponding direction (z) was taken normal to the heme plane, as indicated in the X-ray determined structure of aquo-ferric hemoglobin, and bisecting the H—O—H angle of 104.5°, as found in neutron diffraction determined structures of $3d$ transition metal-ion hydrates. Ladner et al. (1977) take the water oxygen-iron distance to be 1.99 Å on the basis of the ionic radii of the ferric ion and oxygen. Oxygen-iron distances are typically in the range 2.0–2.2 Å (Hamilton, 1962). The effect of varying this distance is shown in Fig. 3.

For the $g = 2$ resonance, the orientation (ϕ_{H_2O}) of the plane of the water molecule about the z-direction does not influence the contribution of the water protons to line broadening, but the behavior in the $g = 6$ (xy) plane does depend upon ϕ_{H_2O}, an angle not known at this time. (The x and y directions are defined as in Fig. 2.) Calculations for the $g = 6$ resonance, in which the water molecule has arbitrarily been placed in the yz ($\phi_{H_2O} = 90°$) plane give the following results: for the magnetic field at angles of 0, 30, 60, and 90° with respect to the x axis, the contributions (both protons together) are 63, 50, 35, and 22 $(MHz)^2$, respectively. The phase of these contributions with respect to those shown in Fig. 2 will be known when ϕ_{H_2O} is determined independently (e.g. by neutron diffraction).

EFFECTS OF DEUTERIUM EXCHANGE

When crystals are soaked in mother liquor prepared with D_2O rather than H_2O, or solutions dialyzed against buffer made up with D_2O, many protons are substituted for by deuterons. Complete replacement of protons of class i by deuterons reduces the contribution of this class of nuclear spins to the second moment by $\langle \Delta\nu^2 \rangle_{D_i} / \langle \nu^2 \rangle_{P_i} = g_D^2 I_D(I_D + 1) / g_P^2 I_P(I_P + 1) = 0.0628$, that is, a 94% reduction. (The Fe(III) – Fe(III) broadening is unlikely to be significantly affected by the very small structural changes attending D_2O for H_2O substitution.) H_2O, in the aqueous channels of the protein crystals and bound to the protein and iron, can be essentially totally replaced by D_2O. The readily exchangeable protons of α- and ϵ-amino and other ionizable groups, and of amide (peptide) groups, are quickly replaced by deuterons. There are other protons that exchange slowly (e.g. C2 protons of imidazole rings) and some, imperceptibly slowly (e.g. alkyl protons); these protons, which constitute about half of those belonging to the untreated protein, are not substituted by deuterons during a few days of exposure to heavy-water-based solutions. The processes just described will take place more rapidly in solution than in crystals.

TOTAL SECOND MOMENT, CALCULATED AND OBSERVED

Single Crystals

In Table I are summarized the $g = 2$ calculations of this paper. The sums of the contributions to the second moment of the component lines are 53 (α-iron) and 57 (β-iron) $(MHz)^2$

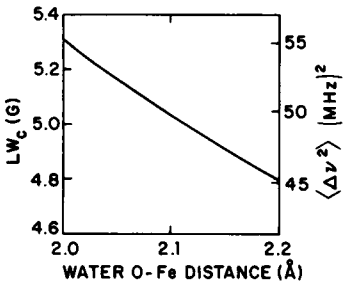

FIGURE 3

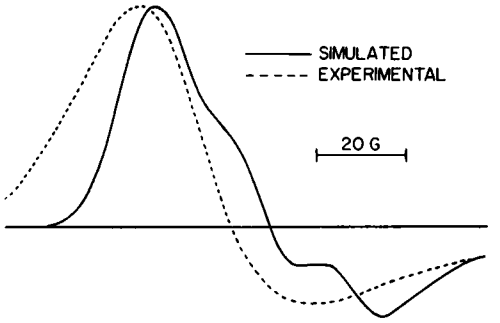

FIGURE 4

FIGURE 3 Line width (peak-to-trough) and total second moment of EPR component hyperfine lines as a function of water oxygen-iron distance, for the $g = 2$ resonance.

FIGURE 4 Low-field EPR spectra at X-band. Solid line: simulated with $g_x - g_y = 0.15$ for one chain and 0.31 for the other, with no spread in the symmetry ratio E/D ($\sigma = 0$). Dashed line: experimental.

(5.2 and 5.4 G) for H_2O, 20 (α-iron) and 25 (β-iron) $(MHz)^2$ (3.2 and 3.6 G) for D_2O. The predicted line narrowing in D_2O is substantial, but cannot be realized experimentally because substitution of D_2O for H_2O in ferric hemoglobin crystals results in more orientation disorder, and it also appears that structural inhomogeneity contributes in a major way to the observed component line widths in these D_2O-treated crystals (Hampton and Brill, 1979).

Hyperfine component line widths at $g = 2$ are available from a companion study (Hampton and Brill, 1979) for comparison with the results given here. In the presence of H_2O, component line widths in crystals are found to be in the range of 4.0–6.0 G, or 31 $(MHz)^2 \leq \langle \Delta\nu^2 \rangle \leq 71$ $(MHz)^2$ for α-, and 4.0–5.5 G or 31–59 $(MHz)^2$ for β-chain irons. Within these ranges are the computed values for $\langle \Delta\nu^2 \rangle$ just given. The agreement of the

TABLE I

CONTRIBUTIONS TO THE SECOND MOMENT OF EPR COMPONENT HYPERFINE LINES AT $g = 2$ FROM FERRIC HORSE HEMOGLOBIN CRYSTALS

Source of interaction with ferric ion	Contribution to $\langle \Delta\nu^2 \rangle$			
	H_2O		D_2O	
	α-chain	β-chain	α-chain	β-chain
	MHz^2			
Other ferric ions				
Intratetramer	3.7	3.7	3.7	3.7
Intertetramer	8.4	12.8	8.4	12.8
Protons				
> 10 Å away	0.3	0.3	~0.1	~0.1
< 10 Å, but not on coordinated H_2O or D_2O	7.9	8.0	5.8	6.6
on coordinated H_2O or D_2O*	32.5	32.5	2.0	2.0
Total*	52.8	57.3	20.0	25.2

*Based upon a water oxygen-iron distance of 2.04 Å.

calculated and observed component line widths suggests that all factors involved in crystals have been correctly identified and at least approximately quantitated. It is worth noting that the protons of the H_2O molecule bound to the ferric ion make the greatest contribution to the component line width.

Solutions

If one assumes that the structure of the ferric hemoglobin tetramer is the same in solution as in the crystal, and hence, for example, that the g-tensors obtained from single crystal orientation measurements apply to the molecules in solution, then the total second moment that applies to solution is readily estimated by neglecting the intertetramer ferric-ferric interactions. At $g = 2$, the component line widths calculated in this way are 4.8 G or 44 $(MHz)^2$ in H_2O, and 2.5 G or 12 $(MHz)^2$ in D_2O. The corresponding values arrived at by analysis of frozen solution spectra are 6.1–6.8 G or 73–91 $(MHz)^2$ and 4.5–5.2 G or 40–53 $(MHz)^2$, considerably larger than predicted. In fact, the solution values are as large or larger than those obtained from crystals, whereas, all other factors being the same, the decrease in intertetramer Fe(III)–Fe(III) dipolar broadening in solution must decrease the component line width. One possible explanation is that temporal fluctuations in conformation, proposed to explain other phenomena (Austin et al., 1975; Englander, 1975; Spartalian et al., 1976), get frozen in when the solution is brought to liquid helium temperature, and the distribution in structures gives rise to a distribution in principal g-values and other spin-Hamiltonian parameters. In such case, the values obtained from solution are only "apparent component line widths" since they include the effects of the distribution in spin Hamiltonians. If the calculated component line widths are taken to be correct, the contributions to the apparent component line widths from the spread in spin Hamiltonian parameters are about 4.4 G or 38 $(MHz)^2$ in H_2O and 4.2 G or 34 $(MHz)^2$ in D_2O, equivalent to a spread of 0.13% in $g = 2$. A distribution at $g = 2$ can be related to a distribution at $g = 6$ through the ratio E/D of rhombic to tetragonal components of the zero-field spin-Hamiltonian (Scholes, 1970), as discussed below. Note that the observed differences in second moment between H_2O and D_2O solutions, 33 and 38 $(MHz)^2$ at the ends of the ranges, correspond closely to the calculated difference, 32 $(MHz)^2$.

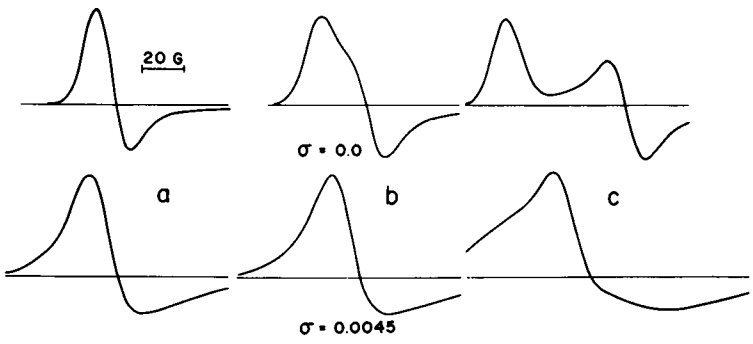

FIGURE 5 Simulated low-field EPR spectra at X-band that demonstrate the influences of a distribution in the symmetry ratio and rhombicity; (*a*) $g_x - g_y = 0$, (*b*) $g_x - g_y = 0.15$, (*c*) $g_x - g_y = 0.31$.

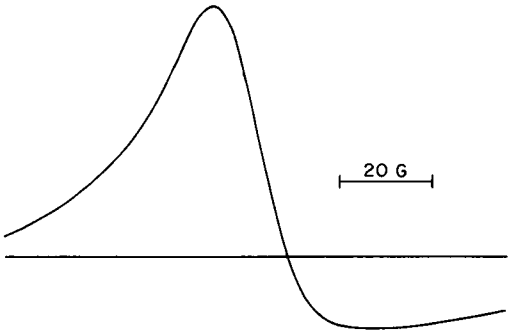

FIGURE 6 Low-field EPR spectrum at X-band simulated with $g_x - g_y = 0.15$ for one chain, 0.31 for the other, and $\sigma = 0.0045$.

SIMULATION OF FROZEN SOLUTION SPECTRA

We assume that the range of apparent component line widths observed in single crystals corresponds to little or no spread in the spin-Hamiltonian parameters at the low end of the range and more at the high end, and that dipolar interactions are the major source of broadening. In frozen solutions, on the other hand, while the average structure is supposed to differ little from that in crystals, the spread in spin-Hamiltonian parameters associated with a distribution in this structure and dipolar broadening appear to have comparable effects. Such an ensemble can be characterized by a function of the symmetry ratio E/D, $\exp-\{[(E/D)_0 - E/D]^2/2\sigma^2\}$, and frozen solution (polycrystalline) spectra simulated on this basis provide a test of the ability of the distributed E/D model to account for the experimental spectrum.

Analysis of the $g = 2$ resonance in frozen solution gives σ in the range 0.0025–0.0045, and single crystal studies show that α- and β-chain g-tensors are somewhat rhombic (Hampton and Brill, 1979). Frozen solution spectra simulated with g tensors of this order of rhombicity are greatly distorted from the experimental spectrum, which appears to be axial (Fig. 4). In Fig. 5 are displayed the low-field regions simulated from single-chain models with $\sigma = 0$ and $\sigma = 0.0045$, with varying degrees of rhombic character. In Fig. 6 is the two-chain spectrum simulated with $\sigma = 0.0045$ and rhombic g-values of Fig. 5. The salient features of the experimental EPR spectrum begin to appear in spectra from rhombic models in which a spread in spin-Hamiltonian parameters has been incorporated. Computer studies are under way to investigate the simulation of frozen solution high-spin ferric hemeprotein spectra as a function of the symmetry ratio, the admixture of triplet states into the ground state, and the width of Gaussian distributions in these parameters (Brill et al., 1978).

We thank Professor M. Perutz and colleagues at the Medical Research Laboratory, Cambridge, England, for providing crystal coordinates in advance of publication (Ladner et al., 1977), and the Protein Data Bank, Brookhaven National Laboratory, Upton, N.Y. for supplying atomic coordinates.

This research was supported by grants from the National Heart, Lung, and Blood Institute (USPHS HL-13989) and the National Science Foundation (PCM 76-83841).

Received for publication 25 March 1978.

REFERENCES

AUSTIN, R. H., K. W. BEESON, L. EISENSTEIN, H. FRAUENFELDER, and I. C. GUNSALUS. 1975. Dynamics of ligand binding to myoglobin. *Biochemistry.* **14**:5355–5373.

BLINDER, S. M. 1960. The hyperfine interaction Hamiltonian. *J. Mol. Spectrosc.* **5**:17–23.

BRILL, A. S., F. G. FIAMINGO, and D. A. HAMPTON. 1978. Characterization of high-spin ferric states in heme proteins. *In* Frontiers of Biological Energetics: Electrons to Tissues. A. Scarpa, J. S. Leigh, Jr., and P. L. Dutton, editors. Academic Press, Inc., New York. Volume 2. 1025–1034.

DICKERSON, R. E., and I. GEIS. 1969. The structure and action of proteins. W. A. Benjamin, Inc., Menlo Park, Calif. 120 pp.

ELLISON, R. O., and H. SHULL. 1955. Molecular calculations. I. LCAO MO self-consistent field treatment of the ground state of H_2O. *J. Chem. Phys.* **23**:2348–2357.

ENGLANDER, S. W. 1975. Measurement of structural and free energy changes in hemoglobin by hydrogen exchange methods. *Ann. N.Y. Acad. Sci.* **244**:10–27.

FEHER, G., R. A. ISAACSON, C. P. SCHOLES, and R. L. NAGEL. 1973. Electron nuclear double resonance (ENDOR) investigation on myoglobin and hemoglobin. *Ann. N.Y. Acad. Sci.* **222**:86–101.

HAMILTON, W. C. 1962. Bond distances and thermal motion in ferrous fluosilicate hexahydrate: a neutron diffraction study. *Acta Crystallogr.* **15**:353–360.

HAMPTON, D. A., and A. S. BRILL. 1979. Crystalline state disorder and hyperfine component line widths in ferric hemoglobin chains. *Biophys. J.* **25**:301–312.

LADNER, R. C., E. J. HEIDNER, and M. F. PERUTZ. 1977. The structure of horse methaemoglobin at 2.0 Å resolution. *J. Mol. Biol.* **114**:385–414.

Löwdin, P-O. 1964. Studies in perturbation theory. VIII. Separation of Dirac equation and study of the spin-orbit coupling and Fermi contact terms. *J. Mol. Spectrosc.* **14**:131–144.

LUZ, Z., and R. G. SHULMAN. 1965. Proton magnetic resonance shifts in aqueous solutions of paramagnetic metal ions. *J. Chem. Phys.* **43**:3750–3756.

PERUTZ, M. F., H. MUIRHEAD, J. M. COX, L. C. G. GOAMAN, F. S. MATHEWS, E. L. MCGANDY, and L. E. WEBB. 1968*a*. Three-dimensional Fourier synthesis of horse oxyhaemoglobin at 2.8 Å resolution: (1) X-ray analysis, *Nature (Lond.).* **219**:29–32.

PERUTZ, M. F., H. MUIRHEAD, J. M. COX, and L. C. G. GOAMAN. 1968*b*. Three-dimensional Fourier synthesis of horse oxyhaemoglobin at 2.8 Å resolution: the atomic model. *Nature (Lond.).* **219**:131–139.

SCHOENBORN, B. P. 1971. A neutron diffraction analysis of myoglobin. III. Hydrogen-deuterium bonding in side chains. *Cold Spring Harbor Symp. Quant. Biol.* **36**:569–575.

SCHOLES, C. P. 1970. EPR studies on heme oriented in an organic crystalline environment. *J. Chem. Phys.* **52**: 4890–4895.

SCHOLES, C. P., R. A. ISAACSON, and G. FEHER. 1972. Electron nuclear double resonance studies on heme proteins. Determination of the interaction of Fe^{3+} with its ligand nitrogens in metmyoglobin. *Biochim. Biophys. Acta.* **263**: 448–452.

SPARTALIAN, K., G. LANG, and T. YONETANI. 1976. Low temperature photodissociation studies of ferrous hemoglobin and myoglobin complexes by Mössbauer spectroscopy. *Biochim. Biophys. Acta.* **428**:281–290.

VAN VLECK, J. H. 1948. The dipolar broadening of magnetic resonance lines. *Phys. Rev.* **74**:1168–1183.

ZHIDOMIROV, G. M., and P. V. SCHASTNEV. 1965. The calculation of the integrals for dipole-dipole hyperfine interaction of electrons with nuclei. *Zh. Strukt. Khim.* **6**:655–656.